AIAA '89

AIAA 89-1018
Analysis & Control of Unsteady Separated Flows

U. Ghia, L. Zuo and K. Ghia,
University of Cincinnati, Cincinnati, OH

AIAA 2nd Shear Flow Conference
March 13-16, 1989 / Tempe, AZ

ANALYSIS AND CONTROL OF UNSTEADY SEPARATED FLOWS†

AIAA-89-1118

U. Ghia*, L. Zuo** and K.N. Ghia*

*Department of Mechanical and Industrial Engineering
Department of Aerospace Engineering and Engineering Mechanics

University of Cincinnati
Cincinnati, Ohio 45221

Abstract

Unsteady separated flow has been studied with the following two major objectives: (1) to develop a methodology for active control, using forced unsteadiness provided by a spoiler flap, and (2) to characterize the development of the separated flow, following the formation and shedding of the starting vortex. An analysis has been developed for simulation of these flows involving temporally deforming boundaries. The Navier-Stokes equations are formulated in time-dependent general orthogonal coordinates which remain boundary aligned for arbitrary boundary deformations. The properties of the coordinates used are exploited to provide high efficiency to the numerical solution procedure. Results obtained for the backstep-channel flow with an oscillating flap provide evidence of the effectiveness of the flap as a control mechanism. The characterization of separation is being carried out using a plane channel with a flap that rises into the oncoming boundary layer.

Introduction

Unsteady flow separation has been the subject of research for several investigations, both experimental (e.g., Refs. 1-3) as well as theoretical (e.g., Refs. 4-6). The efforts are spurred by the interest in high-incidence aerodynamic flows intended to generate high lift but accompanied by repeated vortex formation and shedding. The latter phenomenon itself is exploited via various control maneuvers to maximize lift in burst mode, if not in sustained mode. Towards this goal, the present investigators have examined the flow configuration of a backstep channel with an oscillating flap [7] located in the primary separation zone of this vortex-dominated flow [8]. This theoretical/numerical study is to be coordinated with the corresponding experimental investigations of Nagib and Acharya; the schedule of the experimental facility has not permitted that so far. Nevertheless, some results for this problem are included in the present paper, to demonstrate the effectiveness of the oscillating flap in altering the instantaneous separated-flow features of this configuration.

A focus of the present paper is to analyze the process of separation itself, so that the flow-control mechanism may be triggered appropriately and vehicle control maintained. For this purpose, the simpler configuration of a plane channel with a moveable flap on its lower wall has been examined. For small flap-height to channel-width ratio, this configuration approaches that of a flap on a flat plate - a configuration for which detailed experimental data is expected to be available shortly from Acharya [9].

The problem is formulated using the full time-dependent Navier-Stokes equations in terms of the vorticity ω and the stream function ψ. Direct numerical simulation of the unsteady flow is achieved by direct solution of the stream-function equation using block-Gaussian elimination (BGE) for every time-step advance of the vorticity field using the alternating-direction implicit (ADI) method for the vorticity equation [10]. The coordinate system employed consists of general orthogonal coordinates generated by a generalized conformal mapping [11], with appropriate contraction mappings. The latter serve to map the doubly infinite channel in the physical plane to a bounded region in the computational plane, as well as to appropriately place the uniformly spaced computational-grid points so as to provide resolution of the various length scales in the physical plane. The overall coordinate transformation is capable of generating boundary-aligned coordinates for arbitrary orientation of the flap. To accommodate a moving flap, the coordinate transformation necessarily varies with time. Consequently, the transformation metrics in the flow equations are time-varying. The adverse effect of this on the direct solution of the stream function equation can be significant. However, as described in Refs. [7] and [12], the situation can be very effectively treated by exploiting the properties of conformal mappings, thereby maintaining the efficiency of the ADI-BGE numerical technique.

The physics of vortex-dominated unsteady flow displays widely varying length and time scales. Resolution of these very disparate scales requires an enormously increasing number of grid points as the Reynolds number Re increases, with extremely large computational times. Therefore, direct simulation of such flows for higher Re is faced with computer storage limitations for obtaining accurate resolution of the vorticity field which directly affects the pressure - a parameter conveniently monitored experimentally. The use of a turbulence model may relieve some of these limitations. But the ambiguity associated with

† This research was supported, in part, by AFOSR Grants Nos. 85-0231, 87-0074, in part, by NASA Grant No. NAG-1-753 and, in part, by McDonnell Douglas Grant No. Z71035.

* Professor, Associate Fellow AIAA.
**Graduate Research Assistant.

turbulence modelling raises some concern, specially when characterization of the instantaneous flow field is of interest. It is recognized, however, that this concern is greatest for steady configurations exhibiting unsteady characteristics, i.e., for flows with self-induced unsteadiness. For flows with forced unsteadiness, such as the configurations with a moving flap, the use of a turbulence model can yield meaningful unsteady-flow results, on the time scale of the forced unsteadiness.

Mathematical Formulation

Governing Differential Equations

The time-dependent Navier-Stokes equations expressed in terms of the stream function ψ and vorticity ω with variable effective viscosity ν_e, and time-varying general orthogonal coordinates, can be derived as follows.

Vorticity-Transport Equation

In general vector form and physical time t, the transport equation for vorticity $\bar{\omega}$ is given as

$$\frac{\partial\bar{\omega}}{\partial t} - \bar{\omega}\cdot(\nabla\bar{V}) + \bar{V}\cdot(\nabla\bar{\omega}) = \nabla\times[\nabla\cdot(\nu_e \operatorname{def}\bar{V})] \quad (1)$$

where $$\bar{\omega} = \nabla\times\bar{V} . \quad (2)$$

For 2-D flow in the plane of the unit vectors ($\bar{e}_1$, $\bar{e}_2$) perpendicular to the unit vector $\bar{e}_3$, ω_3 is the only non-zero component of $\bar{\omega}$ and is denoted as ω. For such flow, $\bar{\omega}$ and def $\bar{V}$ can be written as

$$\bar{\omega} = \omega\bar{e}_3 \quad (3)$$

and

$$\operatorname{def}\bar{V} = 2\nabla\bar{V} - \omega(\bar{e}_1\bar{e}_2 - \bar{e}_2\bar{e}_1) . \quad (4)$$

In view of Eq. (4), the RHS of Eq. (1) consists of two major terms; the second of these is considered first. Noting that

$$\nabla\cdot(\nu_e\omega[\bar{e}_1\bar{e}_2 - \bar{e}_2\bar{e}_1]) = \frac{1}{h_2}\frac{\partial}{\partial\xi_2}(\nu_e\omega)\bar{e}_1 + \frac{1}{h_1}\frac{\partial}{\partial\xi_1}(\nu_e\omega)\bar{e}_2, \quad (5)$$

its curl becomes

$$\nabla\times[\nabla\cdot(\nu_e\omega[\bar{e}_1\bar{e}_2-\bar{e}_2\bar{e}_1])] = \frac{1}{h_1h_2}[\frac{\partial}{\partial\xi_1}[\frac{h_2}{h_1}\frac{\partial}{\partial\xi_1}(\nu_e\omega)] + \frac{\partial}{\partial\xi_2}[\frac{h_1}{h_2}\frac{\partial}{\partial\xi_2}(\nu_e\omega)]]\bar{e}_3 \quad (6)$$

To deal with the remaining terms contained within the RHS of Eq. (1), it is noted that

$$\nabla\cdot(\nu_e\nabla\bar{V}) = \nabla\nu_e\cdot\nabla\bar{V} - \nu_e\nabla\times\bar{\omega} , \quad (7)$$

so that, using Eq. (3), the curl of the second term on the RHS of Eq. (7) leads to

$$\nabla\times[\nu_e\nabla\times\bar{\omega}] = -\frac{\bar{e}_3}{h_1h_2}[\frac{\partial}{\partial\xi_1}(\frac{h_2\nu_e}{h_1}\frac{\partial\omega}{\partial\xi_1}) + \frac{\partial}{\partial\xi_2}(\frac{h_1\nu_e}{h_2}\frac{\partial\omega}{\partial\xi_2})] . \quad (8)$$

For the first term on the RHS of Eq. (7), it is noted that, for 2-D flow,

$$\begin{aligned}\nabla\bar{V} = {} & (\frac{1}{h_1}\frac{\partial v_1}{\partial\xi_1} + \frac{v_2}{h_1h_2}\frac{\partial h_1}{\partial\xi_2})\bar{e}_1\bar{e}_1 \\ & + (\frac{1}{h_1}\frac{\partial v_2}{\partial\xi_1} - \frac{v_1}{h_1h_2}\frac{\partial h_1}{\partial\xi_2})\bar{e}_1\bar{e}_2 \\ & + (\frac{1}{h_1}\frac{\partial v_1}{\partial\xi_2} - \frac{v_2}{h_1h_2}\frac{\partial h_2}{\partial\xi_1})\bar{e}_2\bar{e}_1 \\ & + (\frac{1}{h_2}\frac{\partial v_2}{\partial\xi_2} + \frac{v_1}{h_1h_2}\frac{\partial h_2}{\partial\xi_1})\bar{e}_2\bar{e}_2 . \end{aligned} \quad (9)$$

and

$$\nabla\nu_e = \frac{\bar{e}_1}{h_1}\frac{\partial\nu_e}{\partial\xi_1} + \frac{\bar{e}_2}{h_2}\frac{\partial\nu_e}{\partial\xi_2} . \quad (10)$$

Consequently,

$$\nabla\nu_e\cdot\nabla\bar{V} = A_1\bar{e}_1 + A_2\bar{e}_2 \quad (11)$$

where

$$A_1 = \frac{1}{h_1}\frac{\partial\nu_e}{\partial\xi_1}(\frac{1}{h_1}\frac{\partial v_1}{\partial\xi_2} + \frac{v_2}{h_1h_2}\frac{\partial h_1}{\partial\xi_1}) + \frac{1}{h_2}\frac{\partial\nu_e}{\partial\xi_2}(\frac{1}{h_2}\frac{\partial v_1}{\partial\xi_2} - \frac{v_2}{h_1h_2}\frac{\partial h_2}{\partial\xi_1}) \quad (12)$$

and

$$A_2 = \frac{1}{h_1}\frac{\partial\nu_e}{\partial\xi_1}(\frac{1}{h_1}\frac{\partial v_2}{\partial\xi_1} - \frac{v_1}{h_1h_2}\frac{\partial h_1}{\partial\xi_2}) + \frac{1}{h_2}\frac{\partial\nu_e}{\partial\xi_2}(\frac{1}{h_2}\frac{\partial v_2}{\partial\xi_2} + \frac{v_1}{h_1h_2}\frac{\partial h_2}{\partial\xi_1}) . \quad (13)$$

Forming the curl of Eq. (11) completes the derivation of the required expression for the RH: of Eq. (1), which then has the following final form in the computational coordinates (ξ_1,ξ_2,τ):

$$\frac{\partial}{\partial\tau}(h_1h_2\omega) = \frac{\partial}{\partial\xi_1}[(g_{\Omega_1} - \frac{\partial\psi}{\partial\xi_2})\omega]$$

$$- \frac{\partial}{\partial \xi_2}\left[\left(g_{0_2} + \frac{\partial \psi}{\partial \xi_1}\right)\omega\right]$$

$$= -\left[\frac{\partial}{\partial \xi_1}\left(\frac{h_2}{h_1}\frac{\partial}{\partial \xi_1}(\nu_e \omega)\right) + \frac{\partial}{\partial \xi_2}\left(\frac{h_1}{h_2}\frac{\partial}{\partial \xi_2}(\nu_e \omega)\right)\right]$$

$$+ 2\left[\frac{\partial}{\partial \xi_1}\left(\frac{h_2 \nu_e}{h_1}\frac{\partial \omega}{\partial \xi_1}\right) + \frac{\partial}{\partial \xi_2}\left(\frac{h_1 \nu_e}{h_2}\frac{\partial \omega}{\partial \xi_2}\right)\right]$$

$$+ \left[\frac{\partial}{\partial \xi_1}(h_2 A_2) - \frac{\partial}{\partial \xi_2}(h_1 A_1)\right] \qquad (14)$$

where A_1, A_2 are as given by Eqs. (12) and (13), and g_{0_1}, g_{0_2} represent grid-velocity components.

Equation (14) is the required vorticity-transport equation for variable-viscosity flow. It should be noted that, if the fluid viscosity were constant, the last term in the RHS of Eq. (14) vanishes, while the remaining two terms simplify to yield the correct expression for constant-viscosity flow.

Stream-Function Equation

This is obtained by introducing the definition of the stream function, namely,

$$V_1 = \frac{1}{h_2}\frac{\partial \psi}{\partial \xi_2}, \quad V_2 = -\frac{1}{h_1}\frac{\partial \psi}{\partial \xi_1} \qquad (15a,b)$$

into the definition of vorticity given as

$$\omega = \frac{1}{h_1 h_2}\left[\frac{\partial}{\partial \xi_1}(h_2 V_2) - \frac{\partial}{\partial \xi_2}(h_1 V_1)\right]. \qquad (16)$$

Hence, the stream function equation is obtained as

$$\frac{\partial}{\partial \xi_1}\left(\frac{h_2}{h_1}\frac{\partial \psi}{\partial \xi_1}\right) + \frac{\partial}{\partial \xi_2}\left(\frac{h_1}{h_2}\frac{\partial \psi}{\partial \xi_2}\right) = -h_1 h_2 \omega \,. \qquad (17)$$

Boundary Conditions

On the moving flap, the boundary velocity is non-zero, i.e.,

$$\bar{V}_{wall} = V_{w_1}\bar{e}_1 + V_{w_2}\bar{e}_2. \qquad (18)$$

Use of Eqs. (15) and (16) leads to the following conditions for ψ and ω, respectively, at the moving flap:

$$\psi_{wall}\Big|_{\xi_1+\Delta\xi_1} = \psi_{wall}\Big|_{\xi_1} - \int_{\xi_1}^{\xi_1+\Delta\xi_1} h_1 V_{w_2}\, d\xi_1 \qquad (19)$$

and

$$\omega_{wall} = \frac{1}{h_1 h_2}\left[\frac{\partial}{\partial \xi_1}(h_2 V_{w_2}) - \frac{\partial}{\partial \xi_2}(h_1 V_{w_1})\right]_{wall}. \qquad (20)$$

At stationary non-porous walls, the boundary values for ψ and ω are obtainable from Eqs. (19) and (20), with V_{w_2} being set to zero.

The inflow and outflow boundaries are placed at $\xi_1 \to -\infty$ and $\xi_1 \to +\infty$, respectively. The asymptotic form of the governing equations (14) and (17), as $\xi_1 \to \pm\infty$, are solved numerically to determine the values $\omega_\infty(\xi_2)$ and $\psi_\infty(\xi_2)$ at these boundaries.

Initial Conditions

At the boundaries, the initial conditions are exactly the boundary values described in the preceding section. In the interior, the initial conditions are set according to the following relations:

$$\psi^0(\xi_1, \xi_2) = \psi_\infty(\xi_2) \qquad (21)$$

and

$$\omega^0(\xi_1, \xi_2) = \frac{-1}{h_1 h_2}\left[\frac{\partial}{\partial \xi_2}\left(\frac{h_1}{h_2}\frac{\partial \psi_\infty}{\partial \xi_2}\right)\right]. \qquad (22)$$

Thus, the initial distribution for ψ consists of the inflow/outflow boundary values of the stream function, while that for ω corresponds to the asymptotic values scaled by the local metrics.

Outline of Solution Procedure

Following the initial setting up of the mathematical problem, the general solution procedure consists of three major steps:

- Grid generation
- Solution of stream function equation
- Solution of vorticity-transport equation.

These steps are described here briefly; additional details are contained in Refs. [7] and [12].

At each discrete time instant of the unsteady-flow calculation, a boundary aligned coordinate system is generated using a generalized Schwarz-Christoffel conformal mapping technique. These coordinates are appropriately distributed using suitable one-dimensional clustering transformations so as to map the doubly infinite channel configuration to a finite computational region, while simultaneously attempting to provide resolution of the various important length scales of the flow. The conformal mapping varies with time, so as to accommodate the moving flap; the clustering transformations are maintained independent of time, so as to retain the efficiency of the direct-solution procedure used for the stream function equation.

The stream function equation (17) is a Poisson equation and is rearranged such that the differential operator which operates on ψ is time independent, and all the time variation is contained totally within the source term of this Poisson equation. The equation is discretized using central differences and the resulting system of linear coupled algebraic equations is solved

using the direct block-Gaussian elimination (BGE) method developed by Osswald et al. [10].

The temporally parabolic, spatially elliptic vorticity-transport equation is solved very efficiently by an alternating-direction implicit (ADI) technique, with implicit treatment of the wall boundary condition for vorticity. For those cases planned to be tested using turbulence modelling, the Baldwin-Lomax [13] turbulence model is to be employed. It is recognized that the model has deficiencies for the unsteady separated flows under consideration. With careful interpretation of the model, the present investigators have been able to treat small separated regions [14]. In a concurrent effort, various algebraic models as well as differential-equation models are being examined so as to determine if any of these other models perform superior to the Baldwin-Lomax model.

Results and Discussion

Backstep Channel with Control Flap

This configuration (Fig. 1) enables the examination of flow control induced by a surface-mounted flap introducing spanwise vorticity into the separated-flow region. For sufficiently low Reynolds number, a steady-flow separation is observed, and the reattachment length can be significantly reduced via the flap mechanism. As the Reynolds number is increased, spanwise vorticity convected into the separated-flow region is not all convected out of it. This leads to accumulation of vorticity, resulting in a large, spanwise vortex which is eventually shed, carrying the accumulated vorticity with it downstream. The process repeats, and the flow is persistently unsteady, the unsteadiness being enhanced by sympathetic vortex formation and shedding along the upper wall as well. Controlled shedding of the large vortex requires controlled removal of spanwise vorticity from it so as to control the vorticity accumulation inside it. An oscillating flap can serve to achieve this as well. The configuraiton was investigated experimentally by Reisenthal [15]. The Reynolds number values used in the experiment were rather high to enable accurate spatial resolution in the direct numerical simulation. Values of Re up to 32,000 (based on channel width) have been considered in the present work.

Figure 2 shows the instantaneous stream-function contours for the backstep channel, of unit height, with a flap of height 0.25, located at x=1 and oscillating sinusoidally at reduced frequency F=0.16 based on channel height. This frequency corresponds to a reduced frequency of 0.04 based on flap height. The Reynolds number Re, based on channel height, is 2000. Comparison of these results with those obtained previously (Osswald et al. [16]) for the backstep channel without the flap shows that, for example, at Time = 60, the control flap leads to clear reduction in the reattachment length of the primary separation region.

Associated with the control flap are various parameters such as its location and geometry as well as the waveform and frequency of its motion. Of these, the frequency is considered to be the more significant one. Figure 3 shows the results obtained for the case with F=0.25, i.e., a reduced frequency of 0.0625 based on flap height. The length of the primary separation zone is generally smaller than for the case with F=0.16 in Fig. 2.

In order to characterize the formation and shedding of the starting vortex and the separation that follows, the configuration considered is that of a flap that rises up to a designated angle into a boundary layer and then remains stationary until the flow stabilizes. Figures 4 and 5 show the results for such a flap on the lower wall of a plane channel for Re=2000 and 8000, respectively. These values correspond to Re_f=500 and 2000, respectively, based on flap length. The case of Re_f=4000 is shown in Fig. 6. Also, for this last case, the channel width is 8 flap heights, so that Re=32,000, and is intended to better represent the flat-plate configuraiton used in the corresponding experiments of Koga [17] and Acharya [9].

It is necessary to mention, however, that the experiments of Koga [17] are for Re_f=500,000. The computational results described in the present paper have been obtained using direct simulation of the unsteady Navier-Stokes equations, i.e., with no turbulence modeling. As many as (598x51) grid points have been employed in these computations. Even with such refined grids, with the best clustering possible, the direct solutions have been limited to Re_f=4,000. On the other hand, the lowest value of Re_f at which reliable experimental measurements may be possible has been estimated as 10,000 by Acharya [9]. Hence, the numerical analysis and computer code are presently being generalized to accommodate a turbulence model, so that higher values of Re_f may be considered in the computations. At this time, the turbulence model of Baldwin and Lomax [13] is planned to be used. Reviewing Eq. (14), it is observed that the last term on its RHS may not be expressed totally in terms of vorticity alone. The appearance of velocity derivatives in this term further reinforces the $O(\Delta t)$ accuracy of the present calculations. Therefore, effort needs to be directed to improving the temporal accuracy of the numerical scheme as has been done in Ref. [18].

Conclusion

A capability has been developed for numerically simulating 2-D flows in temporally deforming geometries. The procedure depends, in an essential manner, on recognizing that, with time-independent grid clustering, the stream function equation can be rearranged to have a time-independent differential operator, even in the presence of time-varying boundaries. The analysis has been demonstrated via preliminary results obtained for the backstep channel with an oscillating flap as an active flow-control mechanism. The frequency of the flap motion is an important parameter in this mechanism.

Further analysis of the separation process itself is being examined via a flap on a plane-channel wall, approximating flow over a flat plate with a flap. A turbulence model is being incorporated into the analysis so as to obtain solutions for the higher Reynolds numbers used in the experiments.

Seperated flows with forced unsteadiness are far more reproducible than those with self-induced unsteadiness as the latter display chaotic-flow characteristics. The aerodynamic forces associated with unsteady separated flows have peak values many-fold larger, though transient, than those in static configurations. Understanding and control of such flows can play a vital role in achieving such aerodynamic enhancements as needed in supermaneuverability of aircraft.

Acknowledgement

This research is supported by AFOSR Grant 87-0074, under the technical monitorship of Dr. Henry E. Helin.

References

1. Nagib, H.M., Reisenthal, P.H., and Koga, D.J., "On the Dynamical Scaling of Forced Unsteady Separated Flows," AIAA Paper 85-0553, March 1985.

2. Shih, C., Lee, M. and Ho, C-M. "Unsteady Separation Over Two- and Three-Dimensional Airfoils," FJSRL-TR-88-0004, September 1988, pp. 129-135.

3. Luttges, M. and Kennedy, D.A., "Initiation and Use of Three-Dimensional Unsteady Separated Flows," Proceedings of Workshop II on Unsteady Separated Flow, Editors: M. Luttges, M. Robinson and J. Walker, FJSRL-TR-88-0004, September 1988, pp. 211-222.

4. Ghia, K.N., Osswald, G.A., and Ghia, U., "Analysis of Two-Dimensional Flow Past Airfoils Using Unsteady Navier-Stokes Equations," Chapter in Numerical and Physical Aspects of Aerodynamic Flows: Vol. III, Editor: T. Cebeci, Springer Verlag, New York, 1986, pp. 318-340.

5. Osswald, G.A., Ghia, K.N., and Ghia, U., "Simulation of Buffetting Stall for a Cambered Joukowski Airfoil Using a Fully Implicit Method," Lecture Notes in Physics, Editors: F.G. Zhuang and Y.L. Zhu, Springer-Verlag, New York, Vol. 24, pp. 118-132.

6. Visbal, M. and Shang, J., "Numerical Investigation of the Flow Structure Around a Rapaidly Pitching Airfoil," FJSRL-TR-88-0004, September 1988, pp. 91-108.

7. Zuo, L., Ghia, U. and Ghia, K.N., "Numerical Simulation of Control of Separated Flows," Proceeding of AIAA/ASME/ASCE/SIAM/APS 1st NFDC, July 25-28, 1988, Cincinnati, Ohio, AIAA CP-888, pp. 1378-1382.

8. Ghia, K.N., Osswald, G.A. and Ghia, U., "A Direct Method for the Solution of Unsteady Two-Dimensional Incompressible Navier-Stokes Equations," Proceedings of Second Symposium on Numerical and Physical Aspects of Aerodynamic Flows, Long Beach, CA, January, 1983.

9. Acharya, M., Private Communications, 1988.

10. Osswald, G.A. and Ghia, K.N., "Study of Unsteady Incompressible Flow Using Nonuniform Curvilinear Grids, Time Marching, and a Direct Method," Multigrid Methods, NASA CP-2202, 1981, pp.

11. Davis, R.T., "Numerical Methods for Coordinate Generation Based on Schwarz-Christoffel Transformations," AIAA Paper 79-1463, July 1979.

12. Ghia, K.N., Ghia, U. and Osswald, G.A., "Study of Unsteady Separated Viscous Flows and Their Control," FJSRL-TR-88-0004, September 1988, pp. 109-119.

13. Baldwin, B., and Lomax, H., "Thin Layer Approximation and Algebraic Model for Separated Turbulent Flows," AIAA Paper 78-257, 1978.

14. Ramamurti, R., Ghia, U. and Ghia, K.N., "Laminar and Turbulent Flow Through Circular Arc Cascades Using N-S as well as IPNS Formulations," paper under preparation.

15. Reisenthal, P.H., Nagib, H.M. and Koga, D.J., "Control of Separated Flows Using Forced Unsteadiness," AIAA Paper 85-0556, presented at AIAA Shear Flow Conference, Boulder, Colorado, March 1985.

16. Osswald G.A., Ghia K.N. and Ghia, U., "Study of Incompressible Separated Flow Using an Implicit Time-Dependent Technique," AIAA CP 834, 1983, pp. 686-696.

17. Koga, D.J., Nelson, C.F. and Eaton, J.K., "A New Program for Active Control of Unsteady, Separated Flow Structures," FJSRL-TR-88-0004, September 1988, pp. 343-347.

18. Osswald, G.A., Ghia, K.N. and Ghia, U., "A Direct Algorithm for Solution of Incompressible Three-Dimensional Unsteady Navier-Stokes Equations," AIAA CP 874, 1983, pp. 408-421.

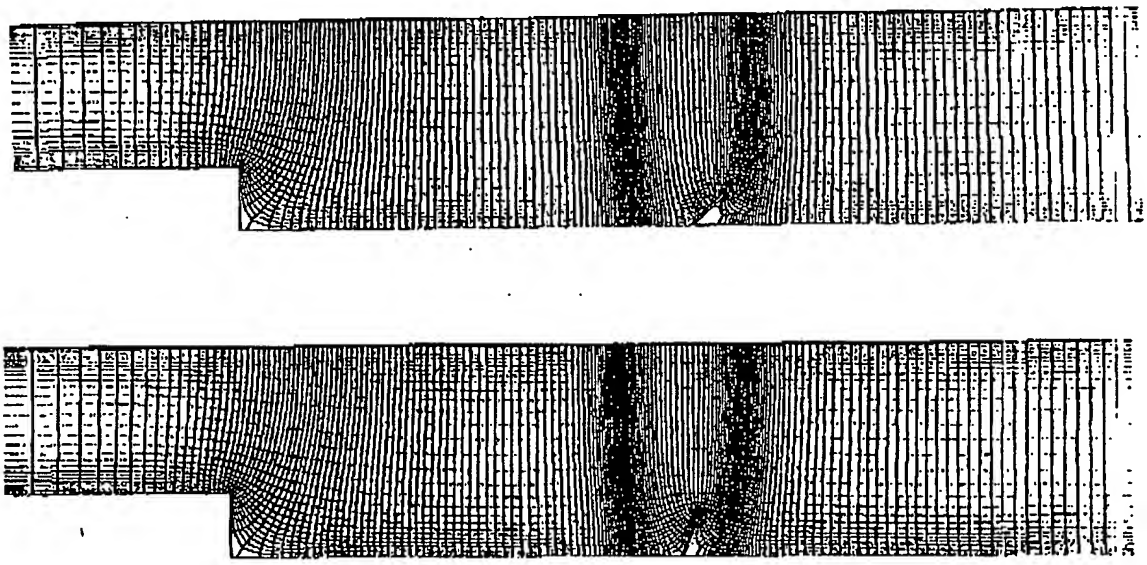

Fig. 1. Clustered Conformal Boundary-Aligned Grid For Backstep Channel With Oscillating Flap In Two Different Positions.

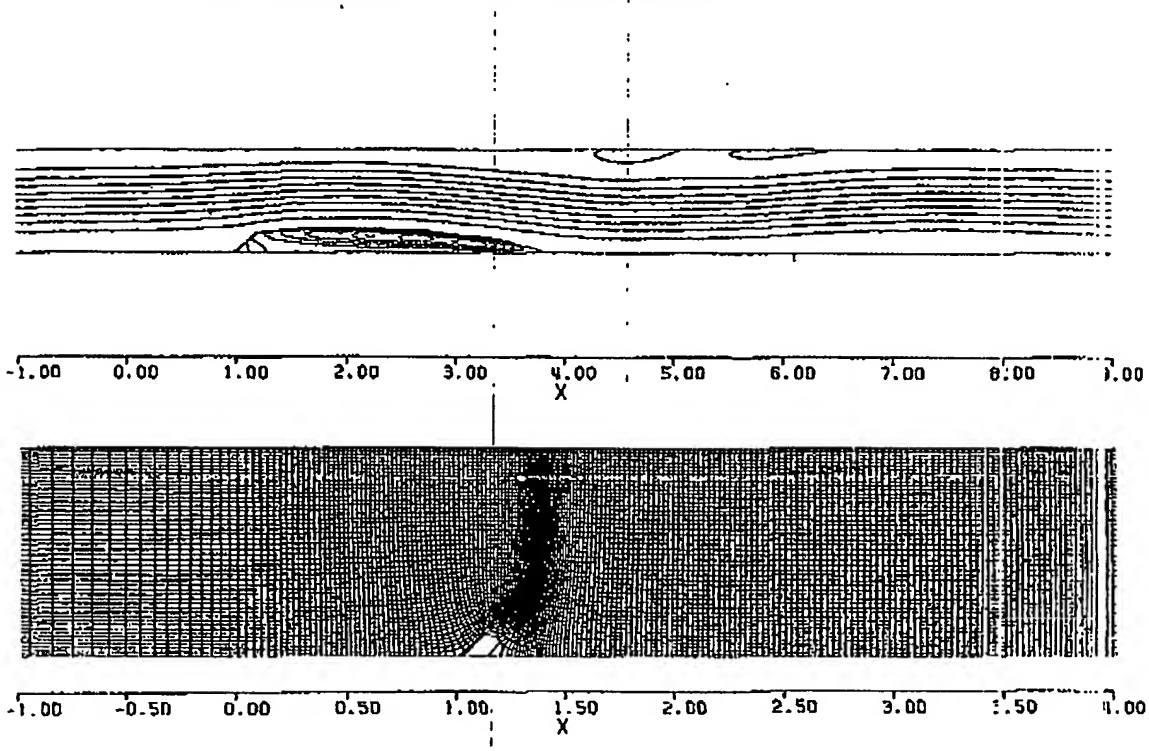

Fig. 4. Flow in Plane Channel With Flap on Lower Wall, Re = 2000, θ = 45°, (499 x 50) Grid, Time = 10.

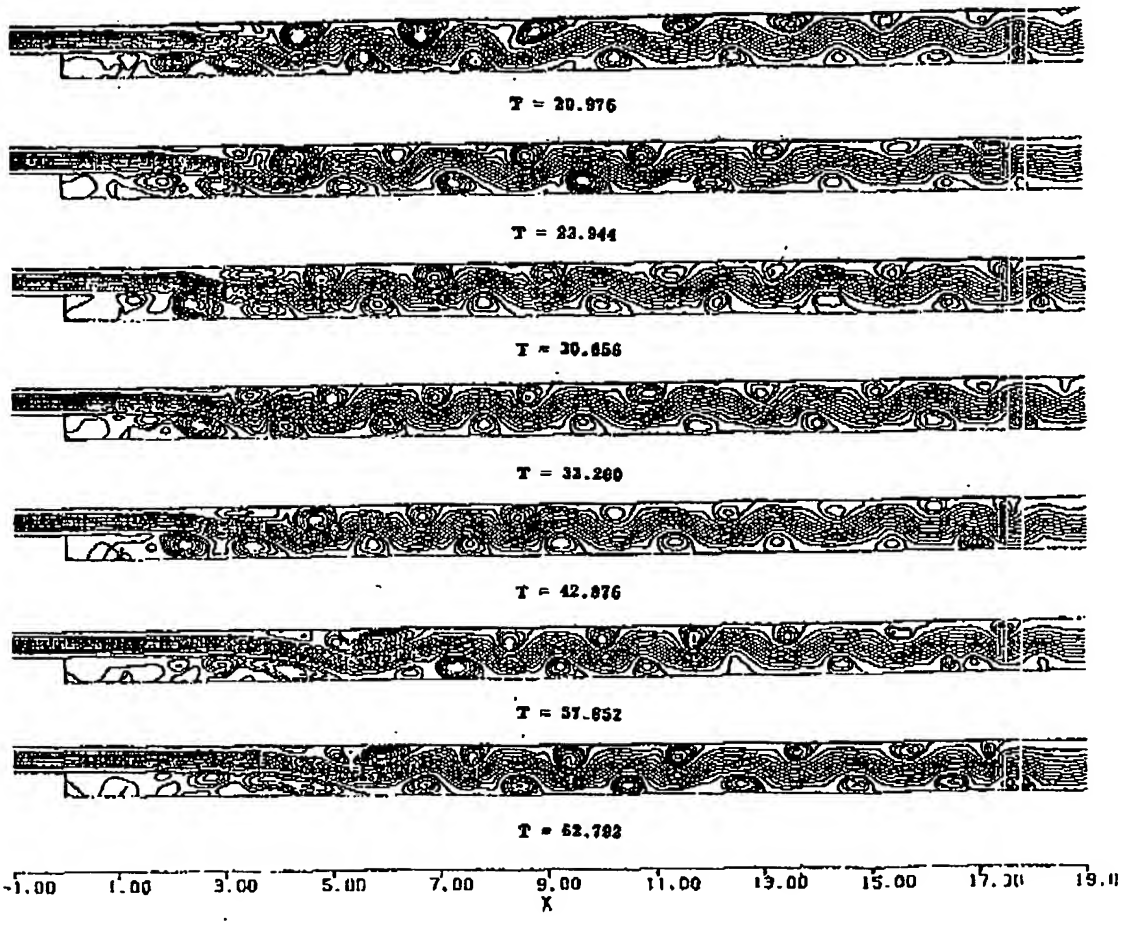

Streamfunction Contours

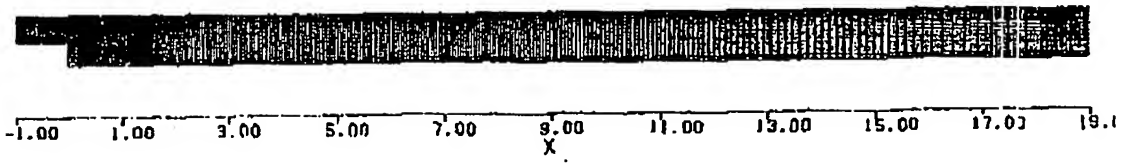

Fig. 2. Unsteady Flow in Back-Step Channel with an Oscillating Flap
Re = 2000, F = .16, 45° < θ < 90°. (375,34)

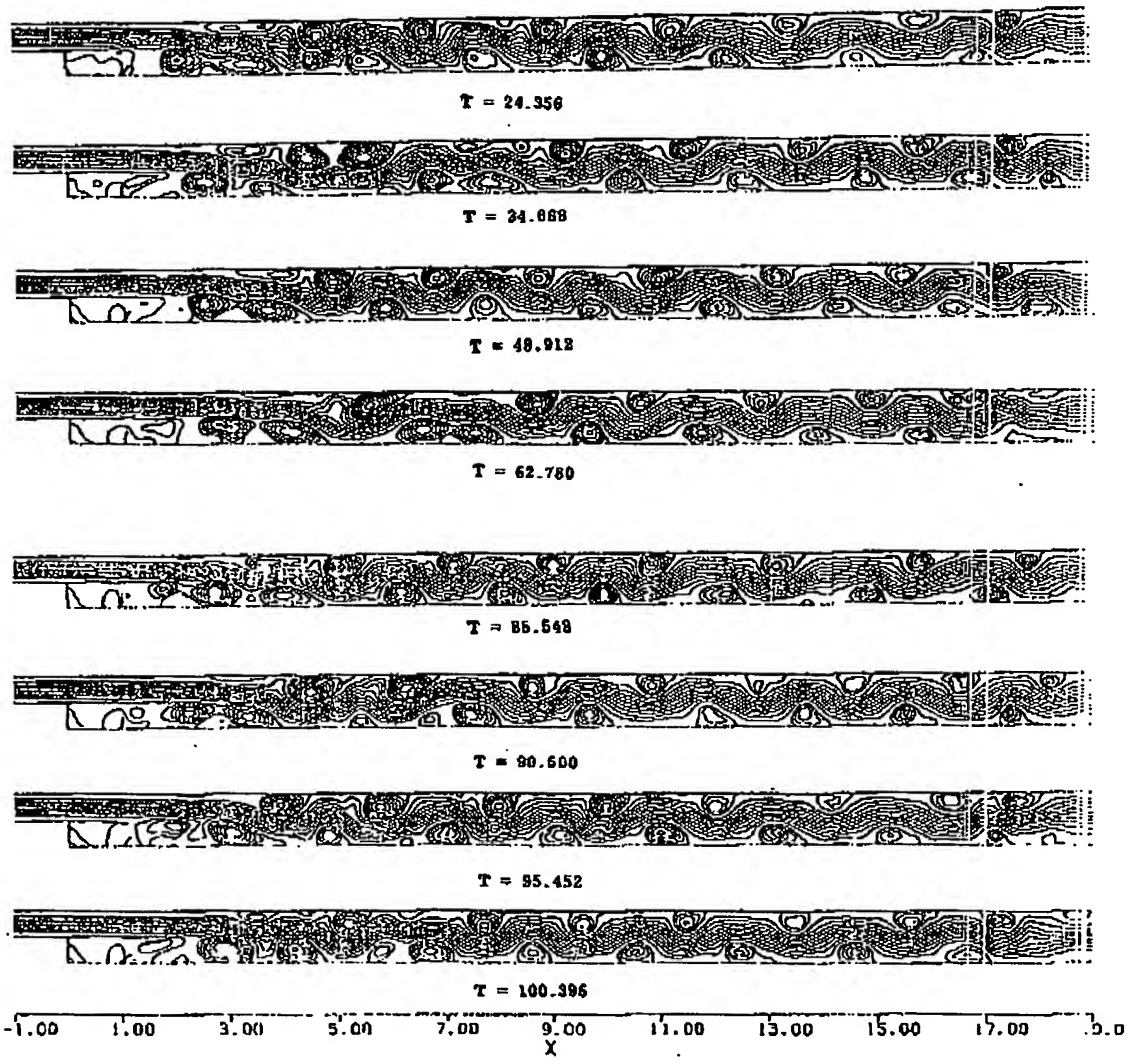

Streamfunction Contours

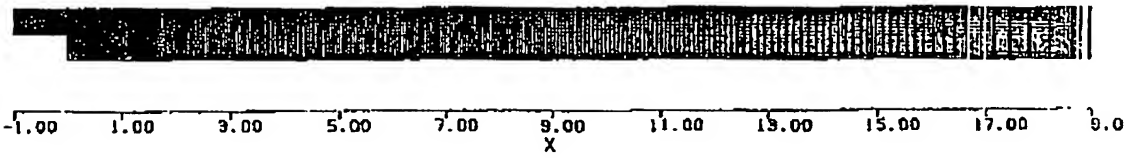

Fig. 3. Unsteady Flow in Back-Step Channel with an Oscillating Flap

Re = 2000, F = .25, 45° < θ < 90°, (375,34)